SINIŠA STANKOVIĆ*#, MARIO DOBRILOVIĆ*, VINKO ŠKRLEC*

OPTIMAL POSITIONING OF VIBRATION MONITORING INSTRUMENTS AND THEIR IMPACT ON BLAST-INDUCED SEISMIC INFLUENCE RESULTS

OPTYMALNE UMIEJSCOWIENIE APARATURY DO MONITOROWANIA DRGAŃ I WIBRACJI ORAZ ICH WPŁYWU NA EFEKTY SEJSMICZNE SPOWODOWANE PRACAMI STRZAŁOWYMI

The major downside of blasting works is blast vibrations. Extensive research has been done on the subject and many predictors, estimating Peak Particle Velocity (PPV), were published till date. However, they are either site specific or global (unified model regardless of geology) and can give more of a guideline than exact data to use. Moreover, the model itself among other factors highly depends on positioning of vibration monitoring instruments. When fitting of experimental data with best fit curve and 95% confidence line, the equation is valid only for the scaled distance (SD) range used for fitting. Extrapolation outside of this range gives erroneous results. Therefore, using the specific prediction model, to predetermine optimal positioning of vibration monitoring instruments has been verified to be crucial. The results show that vibration monitoring instruments positioned at a predetermined distance from the source of the blast give more reliable data for further calculations than those positioned outside of a calculated range. This paper gives recommendation for vibration monitoring instruments positioning during test blast on any new site, to optimize charge weight per delay for future blasting works without increasing possibility of damaging surrounding structures.

Keywords: seismic influence of blasting; peak particle velocity; positioning of vibration monitoring instruments; ground vibration; environmental impact

Jedną z głównych niedogodności związanych z pracami strzałowymi są spowodowane przez te prace wibracje. Problem ten był dogłębnie badany, opracowano także wskaźniki pozwalające na oszacowanie maksymalnej prędkości ruchu cząstek (*Peak Particle Velocity*). Jednakże w większości wskaźniki te są albo globalne (wspólny model niezależny od geologii terenu) lub odnoszące się do specyfiki terenu; dlatego też traktować je należy bardziej jako wytyczne do obliczeń niż dokładne dane. Ponadto, wyniki modelowania uzależnione są, między innymi, od lokalizacji i rozmieszczenia instrumentów do pomiarów i monitorowania drgań oraz wibracji. Przy dopasowaniu danych eksperymentalnych krzywą najlepszego dopasowania i linią obrazującą stopień zaufania na poziomie 95%, okazuje się, że równanie modelu zastosowanie ma jedynie dla skalowanych odległości wykorzystanych w dopasowaniu. Ekstrapolowanie poza ten zakres daje

* UNIVERSITY OF ZAGREB, FACULTY OF MINING, GEOLOGY AND PETROLEUM ENGINEEERING, PIEROTTIJEVA 6, 10000, ZAGREB, CROATIA

Corresponding author: sinisa.stankovic@oblak.rgn.hr

592

wyniki błędne. Dlatego też przed opracowaniem właściwego modelu prognozowania kwestią kluczową jest zastosowanie wstępnego modelu do określenia optymalnej lokalizacji i rozmieszczenia instrumentów pomiarowych. Wyniki wskazują, że rozmieszczenie aparatury pomiarowej we wcześniej wyznaczonej odległości od źródła wybuchu daje bardziej wiarygodne wyniki będące podstawą do dalszych obliczeń niż w przypadku instrumentów umieszczonych poza wyliczonym zakresem. W pracy tej podkreśla się konieczność właściwego umiejscowienia aparatury pomiarowej w trakcie prac strzałowych w nowym miejscu przed przystąpieniem do właściwych obliczeń optymalnej wagi ładunku wybuchowego oraz czasu zwłoki pomiędzy kolejnym strzałami, tak by nie zwiększać ryzyka uszkodzenia sąsiadujących struktur.

1. Introduction

Blasting as a cost-effective energy source for rock breakage is widely used in a number of the mining technologies, geotechnical or civil engineering projects. However, blasting has side effects, environmental impacts, such as ground vibration, air blast, and fly-rock, out of which ground vibration is the most important (Resende et al., 2014). The blast effects include a change in rock behavior having implications on the stability and integrity of structures (Kumar et al., 2016).

The intensity of the seismic effect of blasting can be determined based on the value of measured vibration displacement, velocity, or acceleration.

Commonly accepted standards such as British Standard (BS) 7385, USBM (OSM), etc. are based on the hypothesis that the first assessment of vibration effects should be made before the construction activities. On the other hand, the German Standard DIN 4150 (also accepted as Croatian Standard HRN DIN 4150), based on measured ground vibrations, intends to minimize perceptions and complaints and is not damage based (Mesec et al., 2010).

Various experimental site-specific studies have been performed to develop prediction models. Generally, the peak particle velocity (*PPV*) is presumed a good index for the possibility of damaging surrounding structures (Kumar et al., 2016) since it is linked with the level of stress induced in the structures.

The equations for calculating PPV (peak particle velocity) use scaling distance and/or scaling charge weight per delay, depending on author. One of the commonly used equations for calculating PPV (Siskind, 2000) can be described as:

$$PPV = H(SD)^{-\beta} \tag{1}$$

Where *PPV* is peak particle velocity (mm/s), *SD* (m/kg$^{1/2}$) is square root scaled distance (for cylindrical charge), *H* and *β* are site factors that are calculated from performed blasts.

Scaling of distance *SD* (equation 2) is necessary to predict velocities when both the charge weight per delay, *W*, and the distance, *R*, vary. The two most popular approaches are the square root, $R/W^{1/2}$, scaling and cube root, $R/W^{1/3}$, scaling (Dowding, 1985). In this research square root scaling distance is used.

$$SD = \frac{R}{\sqrt{W}} \tag{2}$$

Where *SD* is square root scaling distance (m/kg$^{1/2}$), *R* is distance from measurement point to the blast (m), *W* is charge weight per delay (kg).

In the absence of field blast data, empirical models are used to evaluate these constants (Kumar et al., 2016).

Many authors have published their site-specific studies presenting models equivalent to equation (1). Nicholson in his Master Thesis (Nicholson, 2005) presented his prediction model gained from blasting works in Bengal Quarry. Ozer presented different models for different regions and geological conditions within "Istanbul, Kadikoy-Kartal Railway Mass Transport System" project (Ozer, 2008). ISEE gave the equation for the upper-bound line for Typical Data From Downhole Blasting (ISEE, 1998). A study in magnesite mine, (Ak et al., 2009) presented PPV prediction equation representing 95% confidence level. In his Thesis "Blast vibration studies in surface mines" Badal presented PPV Predictor Equation for the Jindal Power Open Cast Coal Mine (Badal, 2010). Mesec based his research on several test sites in sediment rock deposits comprising mainly of limestone and dolomite, with different geological strength index (GSI) values (Mesec et al., 2010).

In contrast to conventional way of PPV prediction, Rai et al. (Rai et al., 2005) studied the prediction of maximum safe charge per delay in surface mining by collecting a wide variety of vibration data obtained from different mines in limestone and sandstone formations and compared the proposed equation with the PPV predictor equations in the literature (Ak et al., 2009).

Today, most of the published papers regarding vibration velocity measurements are based on large amount of data collected during certain project or quarry exploitation and analyzed through statistical approach or neural networks (Monjezi et al., 2010). In a view of short-term projects i.e. open pit excavation in rock for underground parking or open cut for road or highway, the principle is slightly different. Measurements from one trial blast need to give the regime of blasting for the whole project. Maximum charge weight per delay for test blast is usually calculated from one of the empirical prediction models. With that charge weight per delay, a test blast is carried out, and vibration velocity is recorded at several measurement points. From recorded data, calculations are made to produce blasting regime for future productive blasting.

Since the calculated model among other factors highly depends on positioning of vibration monitoring instruments, when fitting of experimental SD – PPV data to equation (1) it gives the coefficients H and β, which are valid only for the SD range used for fitting. Extrapolation outside of this range gives erroneous results.

Usually, measurement instruments are positioned near, on the base ground, or directly on foundations of structure of interest. Therefore, it will give valid data only for that area and distance from the blast at the time of measurement. When blasting works will expand towards mentioned structures of interest, the equation gained from calculations will give largely reduced permitted charge weight per delay.

To be sure to get usable measurement data, optimal positioning of the vibration monitoring instruments is imperative.

However, there is no published recommendation for vibration monitoring instruments positioning during test blast on any new site. For this purpose, on-site experimental research has been carried out, with variation of only one parameter, the distance R from measurement point to the blast. The result of this research gives the end user the certainty of getting fully usable measurement data and consequently optimal and safer blasting works.

2. The test site

For the research location, a quarry near Zadar has been selected. The quarry was chosen because of its specific geological conditions in order to obtain measurements and calculations for real conditions of the rock mass.

The quarry „Busišta 2" is located around 4 km NE of the village of Smilčić and around 1 km north of the road Smilčić-Karin, on a hillside slightly sloped towards NE between 140 m and 165 m of altitude. The lowest altitude is on the NE and highest on the SW. The quarry is a part of a NE wing of Cretaceous-Paleogene anticline. Foraminiferal limestone deposits have a NE slope under 20° angle. Basic structural and tectonic fabric of this area was formed in Middle Eocene (Istrian-Dalmatian orogenesis phase). During that time, the folding of Cretaceous and Paleogenic sediments occurred. Well layered limestone has a very light slope (up to 10°) towards NE. The fracture system in the quarry is relatively dense, with two predominate orientations. The first fracture set are longitudinal clefts (vertical fractures) with the slope generally opposite to the slope of the deposits. The second fracture set has the slope parallel to the slope of the deposits. Both fracture sets are subvertical to vertical. At certain places of open-faced profiles, there are visible fractures in one package of layers, while the layers just above and below are undisturbed. That implies that the fractures were developed just after the deposition of said package of layers. Nevertheless, majority of the fractures are the result of tectonic activity of the quarry region during and after the folding (IGI, 1967).

The geological conditions of the testing site are shown in Figure 1, and its physical-mechanical properties in Table 1. The testing micro-locations within quarry presented in Figure 2, were defined along the exploitation bound not to disturb the ongoing work in the quarry in any way.

Prior to the field test blast, a model for optimal positioning of vibration monitoring instruments has been chosen, to get more precise and usable measurements for further analysis.

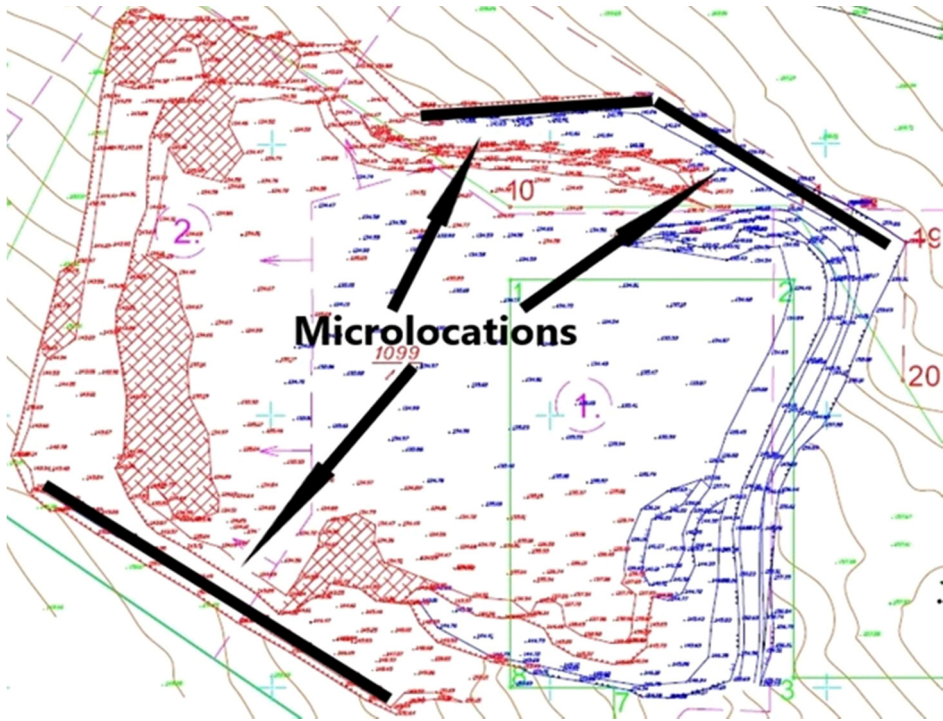Fig. 1. Typical geology of testing site (top 5 m of the slope)

Fig. 2. Topographic view of testing site with testing micro locations

Physical-mechanical properties of rock

Rock property	Symbol	Units	Test results	
			Range	Median
Uniaxial strength (in dry condition) (HRN B.B8.012:1987)	R	MPa	121-166	142
Water absorption (HRN B.B8.010:1980)	U	% (mas)	0.53-0.90	0.69
Apparent density (HRN B.B8.032:1980)	ρ_b	g/cm^3	2.58-2.62	2.61
Open porosity (HRN B.B8.032:1980)	p_O	% (vol)	1.40-2.32	1.80

3. Prediction models

Prediction models described in introduction have been collected and equations with square root scaling distance and 95% confidence line equation are presented in Figure 3 and Table 2.

In Ozer's research (Ozer, 2008) the project have been divided in 6 regions with different geology. The equation from region 5 was used because it is the region with only one type of limestone (GSI 55-60). The equation was developed during 61 blasts with total of 114 recorded events. Ak et al. developed equation during 43 blasts with 43 recorded events (Ak et al., 2009). Mesec et al. research has been divided in three groups with different GSI value. Equation from

596

group III was used because it is limestone material (GSI 51-55) and developed from 92 recorded events in total, out of which 29 recorded events were from test blasting (Mesec et al., 2010).

Since all the prediction models were developed during blasting works in different site-specific condition, site constants H and β vary from 186 to 1367 for H and from 0.81 to 1.59 for β (Table 2) which can also be concluded from regression curves shown in Figure 3. As expected, the largest differences are closer to the blast and can differ up to three times (lowest value gives Ozer and highest Mesec et al. prediction model). Furthermore, the differences are also in distance of measurement instruments from the blast and corresponding principal frequencies (Table 3).
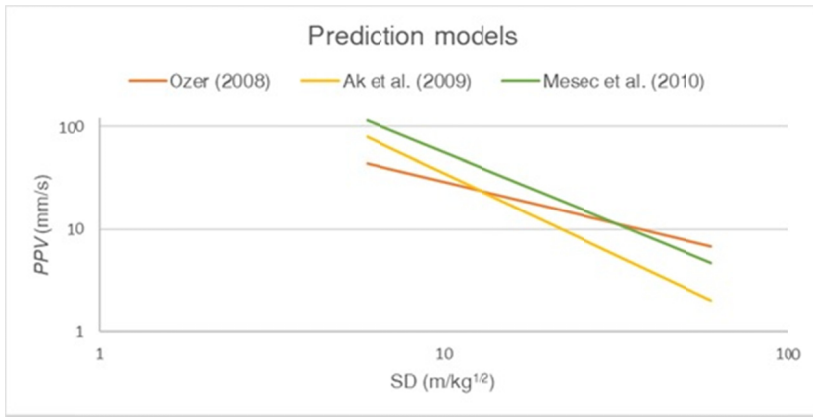

Fig. 3. Graphical presentation of results of prediction model equations

TABLE 2

Summary of prediction models

No.	Researchers	Empirical models
1	Ozer (2008) (limestone-region 5)	$PPV = 186(SD)^{-0.81}$
2	Ak et al. (2009)	$PPV = 1367(SD)^{-1.59}$
3	Mesec et al. (2010) (group III)	$PPV = 1349(SD)^{-1.38}$

TABLE 3

Distance from the blast and principal frequency data from different researchers

No.	Researchers	Distance from the blast (m)	Principal frequency (Hz)
1	Ozer (2008) (limestone-region 5)	32-367	24-100
2	Ak et al. (2009)	198-1280	1.9-46.5
3	Mesec et al. (2010) (group III)	1.8-78 (1.8-29.8 during test blasts)	8-87

For further calculations prediction model developed by Mesec et. al. (Mesec et al., 2010) has been chosen due to two reasons:
1. The research has been done in similar geological conditions;
2. Part of the presented data from research were from test blasts.

4.   Seismic effect of blasting and test blast

The intensity of the seismic effect of blasting can be determined based on the values of measured oscillations displacement, velocity, or acceleration.

Croatian Standard HRN DIN 4150, 1-3:2011 (Croatian Standards Institute, 2011) accepts vibration velocity as an assessment of the negative effects of blasting on the environment or surrounding structures. Hence, the intensity of the seismic effect of blasting is determined by measuring vibration velocity. The Standard recognizes three types of structures: industrial buildings, residential buildings, and delicate constructions. It also determines the vibration velocity limits for each, in relation to the principal frequency.

To determine optimal positioning of vibration monitoring instruments, peak particle velocity limits must be selected. As there are no populated areas surrounding quarry, the PPV limit was taken for industrial buildings. Since principal frequency cannot be predicted, both minimum and maximum limits were used (20 mm/s-50 mm/s). The scaling distances have been calculated using chosen *PPV* limit values in empirical model equation by Mesec et al. (Fig. 4). To predetermine positions for vibration monitoring instruments, distance *R* has been calculated from the scaling distance equation (equation 2). Both are presented in Table 4.
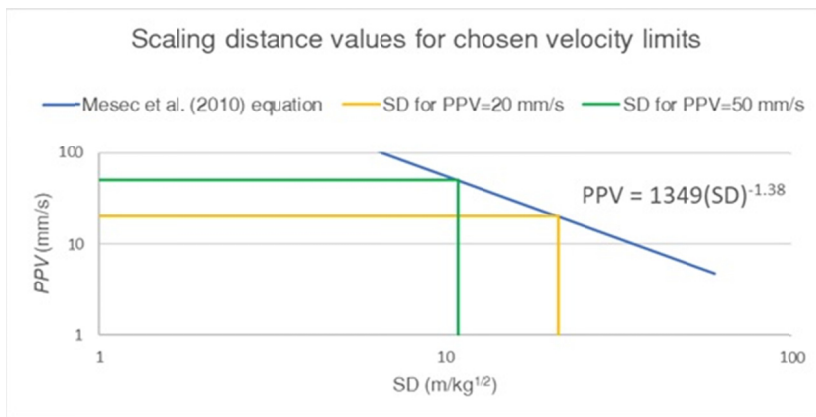

Fig. 4. Graphical presentation of scaling distance values for chosen velocity limits

Instruments were installed in measurement line between 1.5 m and 80 m distance during 17 blast with total of 122 recorded events, to cover larger area than calculated for further analysis and discussion.

TABLE 4

Calculated values of scaling distances (*SD*) and distances (*R*) for chosen velocity limits

Velocity (mm/s)	SD (m/kg$^{1/2}$)	R (m)
50	10.9	18.1
20	21.1	35.2

Since the diameter of the drill holes undoubtedly influences the seismic effects of a blast (Kuzmenko et al., 1993), all drilled holes were identical, 89 mm in diameter and 3 m deep, with no free surface (confined). To guarantee equivalent conditions during measurements, explosive used was of the same type, diameter, and gross mass. The explosive was a single cartridge of ELEXIT-2 per hole, with following specifications: 590 mm in length, 65 mm diameter, gross mass of 2.778 kg, density of 1400 kg/m^3, velocity of detonation 5500 m/s, energy release of 4500 kJ/kg and gases volume of 851 l/kg (MAXAM Hrvatska d.o.o., 2010).

The vibration monitoring instruments used during this research were INSTANTEL BlastMate Series II and III, INSTANTEL Minimate and INSTANTEL Minimate plus. General specifications for vibration monitoring instrument INSTANTEL Minimate Plus are presented in Table 5. The instrument installation during measurement and typical blasting and measurement setup are shown in figures 5 and 6.

TABLE 5

General specifications for vibration monitoring instrument INSTANTEL Minimate Plus (Instantel Inc, 2013)

General Specifications - Minimate Plus	
Vibration monitoring (with Standard Triaxial Geophone)	
Range	Up to 254 mm/s (10 in/s)
Resolution	0.127 mm/s (0.005 in/s)or 0.0159 mm/s (0.000625 in/s) with built-in preamp
Accuracy (ISEE/DIN)	+/- 5% or 0.5 mm/s (0.02 in/s), whichever is larger, between 4 and 125 Hz / DIN 45669-1 standard
Transducer Density	2.13 g/cc (133 lbs/ft^3)
Frequency Range (ISEE/DIN)	2 to 250 Hz, within zero to -3 dB of an ideal flat response / 1 to 315 Hz
Maximum Cable Length (ISEE/DIN)	75 m (250 ft) / 1000 m (3280 ft)

Fig. 5. The vibration monitoring instrument installation during measurement at closest point (1.5 m)
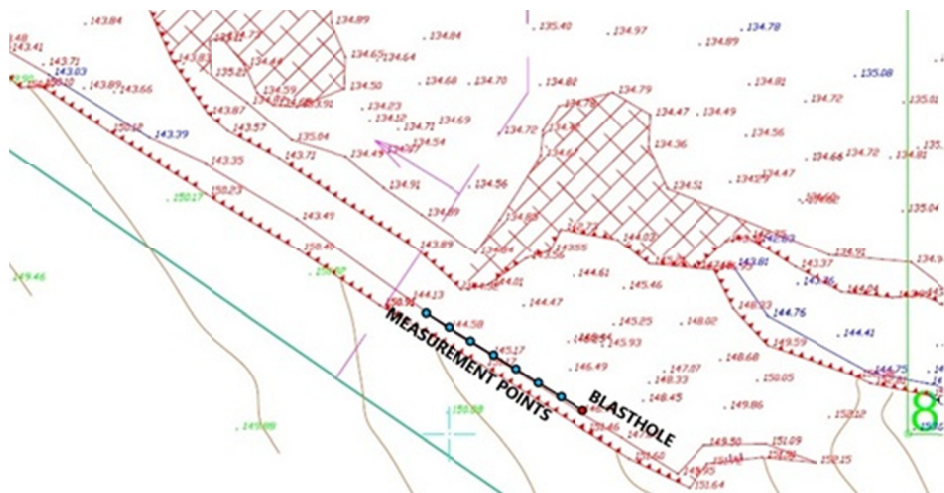
Fig. 6. Typical blasting and measurement setup

5.   Results and discussion

Obtained field measurement data are downloaded and processed using the Instantel software "Blastware", release 10.74 (Instantel Inc, 2004). As a result, an event record for all 122 measuring points is created.

The main objective of using predetermined measurement positions is to get the most accurate and usable data for later analysis.

To validate the importance of positioning instruments for test blast, measured data was divided in four sections: distance range calculated from empirical model equation (18 m-35 m), distances over 35 m, over 40 m and over 45 m from the blasthole. Since software automatically accepts only valid measurements (measurements with measured value within instrument range limits), 4 measurements with measured value that exceeds instrument range limit (>254 mm/s) are discarded. Additionally, measurements closer than calculated range were discarded as well from future calculations due to measured PPV values exceeds maximum selected PPV limit, hence they are not vital for this research. Regardless, all data are shown in graphical presentation (Fig. 13) and full record listing is given in Figure 7. Sample of the event report is given in Figure 8. For each section 95% confidence line equation is presented in Table 6 and Figures 9-14, which shows that, depending on vibration monitoring instrument positions, a difference in results occurs. The largest differences are closer to the source of explosion.

Taking into consideration that majority of principal frequency values lies between 50 and 65 Hz, from DIN 4150 standard a 40 mm/s PPV limit has been chosen. By comparing scaling distance for each section equation for the same charge weight per delay (2,778 kg) and velocity of 40 mm/s (Table 7 and Fig. 15) the results differ from 13.4 m/kg$^{1/2}$ to 25.0 m/kg$^{1/2}$.

Implementing equations for each section in further calculations for permitted charge weight per delay in relation to distance from the blast for peak particle velocity limit of 40 mm/s, the results show that each section that is further away, gives lower values for permitted charge weight per delay (Table 8).

600

Listing of SVE.SDF Records

Serial No.	Date/Time	Tran Peak (mm/s)	Vert Peak (mm/s)	Long Peak (mm/s)	Mic Peak (pa./dB)	Back Ground (pa./dB)	Weight (kg)	Distance (m)	Description
B3-MP4	Feb 9 /11 13:55:13	9.779	21.84	17.65	0.000	0.000	2.778	20.00	Zadar
B3-MP6	Feb 9 /11 13:56:13	4.064	11.18	15.24	0.000	0.000	2.778	30.00	Zadar
B4-MP4	Feb 9 /11 13:57:13	10.67	10.54	9.779	0.000	0.000	2.778	25.00	Zadar
B4-MP6	Feb 9 /11 13:57:13	3.302	5.334	9.779	0.000	0.000	2.778	35.00	Zadar
B5-MP4	Feb 9 /11 13:59:13	8.763	5.461	9.906	0.000	0.000	2.778	30.00	Zadar
B5-MP6	Feb 9 /11 13:59:13	3.683	4.318	8.636	0.000	0.000	2.778	40.00	Zadar
B3-MP7	Feb 9 /11 14:00:14	15.62	11.56	32.13	0.000	0.000	2.778	35.00	Zadar
B4-MP7	Feb 9 /11 14:01:14	14.60	6.604	24.00	0.000	0.000	2.778	40.00	Zadar
B3-MP1	Feb 9 /11 14:02:14	107.7	0.000	95.50	0.000	0.000	2.778	5.000	Zadar
B4-MP1	Feb 9 /11 14:03:14	21.59	36.58	36.58	0.000	0.000	2.778	10.000	Zadar
B3-MP3	Feb 9 /11 14:03:14	10.67	31.50	27.43	0.000	0.000	2.778	15.00	Zadar
B5-MP7	Feb 9 /11 14:03:14	9.525	5.334	21.21	0.000	0.000	2.778	45.00	Zadar
B3-MP2	Feb 9 /11 14:04:14	69.21	53.85	58.55	0.000	0.000	2.778	10.000	Zadar
B4-MP3	Feb 9 /11 14:05:14	5.461	13.97	8.890	0.000	0.000	2.778	20.00	Zadar
B5-MP1	Feb 9 /11 14:05:14	20.83	13.97	6.350	0.000	0.000	2.778	15.00	Zadar
B3-MP5	Feb 9 /11 14:05:14	4.953	14.99	17.65	0.000	0.000	2.778	25.00	Zadar
B4-MP2	Feb 9 /11 14:06:14	35.05	28.32	15.62	0.000	0.000	2.778	15.00	Zadar
B5-MP3	Feb 9 /11 14:07:14	6.604	7.874	9.398	0.000	0.000	2.778	25.00	Zadar
B4-MP5	Feb 9 /11 14:07:14	3.302	8.128	8.255	0.000	0.000	2.778	30.00	Zadar
B5-MP2	Feb 9 /11 14:08:14	14.35	13.21	9.906	0.000	0.000	2.778	20.00	Zadar
B5-MP5	Feb 9 /11 14:09:14	2.667	4.191	6.350	0.000	0.000	2.778	35.00	Zadar
B3-MP8	Feb 9 /11 14:00:14	5.334	8.636	13.97	0.000	0.000	2.778	40.00	Zadar
B4-MP8	Feb 9 /11 14:01:14	3.683	4.064	12.45	0.000	0.000	2.778	45.00	Zadar
B5-MP8	Feb 9 /11 14:03:14	3.048	2.667	12.19	0.000	0.000	2.778	50.00	Zadar
B1-MP2	Jan 17 /11 10:19:10	11.68	55.88	47.75	0.000	0.000	2.778	10.000	Zadar
B2-MP2	Jan 17 /11 10:21:10	8.636	41.66	21.34	0.000	0.000	2.778	14.50	Zadar
B1-MP1	Jan 17 /11 10:32:10	39.24	172.6	160.7	0.000	0.000	2.778	5.000	Zadar
B1-MP5	Jan 17 /11 10:33:10	12.32	9.271	6.604	0.000	0.000	2.778	30.00	Zadar
B2-MP1	Jan 17 /11 10:35:10	11.43	30.10	26.03	0.000	0.000	2.778	9.500	Zadar
B2-MP5	Jan 17 /11 10:36:10	7.620	5.588	4.699	0.000	0.000	2.778	34.50	Zadar
B1-MP6	Jan 17 /11 10:37:10	10.92	8.890	9.779	0.000	0.000	2.778	35.00	Zadar
B1-MP4	Jan 17 /11 10:40:10	15.11	26.54	20.07	0.000	0.000	2.778	25.00	Zadar
B1-MP3	Jan 17 /11 10:40:10	16.51	22.99	26.16	0.000	0.000	2.778	15.00	Zadar
B2-MP6	Jan 17 /11 10:40:10	10.29	6.858	11.94	0.000	0.000	2.778	39.50	Zadar
B2-MP4	Jan 17 /11 10:43:10	16.00	17.53	21.84	0.000	0.000	2.778	29.50	Zadar
B2-MP3	Jan 17 /11 10:43:10	18.03	15.49	30.10	0.000	0.000	2.778	19.50	Zadar
B1-MP7	Jan 17 /11 10:37:10	4.191	7.112	6.477	0.000	0.000	2.778	40.00	Zadar
B2-MP7	Jan 17 /11 10:40:10	4.064	5.715	5.207	0.000	0.000	2.778	44.50	Zadar
B6-MP7	Mar 23 /11 18:07:18	8.255	7.493	14.99	0.000	0.000	2.778	35.00	Zadar
B7-MP7	Mar 23 /11 18:09:18	9.017	4.191	13.21	0.000	0.000	2.778	40.00	Zadar
B8-MP7	Mar 23 /11 18:11:18	7.239	3.302	12.70	0.000	0.000	2.778	45.00	Zadar
B6-MP2	Mar 23 /11 18:11:18	35.56	32.51	60.96	0.000	0.000	2.778	10.000	Zadar
B7-MP2	Mar 23 /11 18:13:18	23.37	10.16	33.53	0.000	0.000	2.778	15.00	Zadar
B6-MP1	Mar 23 /11 18:14:18	38.35	151.4	65.66	0.000	0.000	2.778	5.000	Zadar
B8-MP2	Mar 23 /11 18:15:18	25.91	19.30	39.62	0.000	0.000	2.778	20.00	Zadar
B6-MP4	Mar 23 /11 18:16:18	14.22	13.46	27.43	0.000	0.000	2.778	20.00	Zadar
B7-MP1	Mar 23 /11 18:16:18	17.78	27.30	27.30	0.000	0.000	2.778	10.000	Zadar
B6-MP5	Mar 23 /11 18:17:18	17.53	15.24	21.97	0.000	0.000	2.778	25.00	Zadar
B8-MP1	Mar 23 /11 18:18:18	16.89	27.69	22.48	0.000	0.000	2.778	15.00	Zadar
B7-MP4	Mar 23 /11 18:18:18	11.18	7.874	21.34	0.000	0.000	2.778	25.00	Zadar
B6-MP3	Mar 23 /11 18:19:18	40.39	50.67	36.45	0.000	0.000	2.778	15.00	Zadar
B6-MP6	Mar 23 /11 18:19:18	6.985	6.223	15.87	0.000	0.000	2.778	30.00	Zadar
B8-MP4	Mar 23 /11 18:19:18	7.874	6.604	21.59	0.000	0.000	2.778	30.00	Zadar
B7-MP5	Mar 23 /11 18:20:18	9.271	11.81	18.67	0.000	0.000	2.778	30.00	Zadar
B8-MP5	Mar 23 /11 18:21:18	4.064	10.80	16.38	0.000	0.000	2.778	35.00	Zadar
B7-MP3	Mar 23 /11 18:21:18	20.57	18.92	11.05	0.000	0.000	2.778	20.00	Zadar
B7-MP6	Mar 23 /11 18:21:18	5.588	3.937	13.59	0.000	0.000	2.778	35.00	Zadar
B8-MP3	Mar 23 /11 18:22:18	21.84	10.79	14.22	0.000	0.000	2.778	25.00	Zadar
B8-MP6	Mar 23 /11 18:23:18	4.191	3.048	12.19	0.000	0.000	2.778	40.00	Zadar
B6-MP8	Mar 23 /11 18:07:18	8.255	3.683	10.41	0.000	0.000	2.778	40.00	Zadar
B7-MP8	Mar 23 /11 18:09:18	6.223	2.540	5.588	0.000	0.000	2.778	45.00	Zadar
B8-MP8	Mar 23 /11 18:11:18	3.683	2.159	6.604	0.000	0.000	2.778	50.00	Zadar
B9-MP7	Apr 6 /11 11:43:11	7.366	5.080	12.06	0.000	0.000	2.778	35.00	Zadar
B10-MP7	Apr 6 /11 11:45:11	6.096	4.699	11.43	0.000	0.000	2.778	40.00	Zadar
B11-MP7	Apr 6 /11 11:47:11	6.858	5.080	12.57	0.000	0.000	2.778	45.00	Zadar
B9-MP4	Apr 6 /11 11:48:11	21.59	9.906	19.30	0.000	0.000	2.778	20.00	Zadar
B10-MP4	Apr 6 /11 11:50:11	8.128	4.763	11.43	0.000	0.000	2.778	25.00	Zadar
B9-MP3	Apr 6 /11 11:51:11	28.83	10.67	31.88	0.000	0.000	2.778	15.00	Zadar
B11-MP4	Apr 6 /11 11:52:11	6.604	3.048	14.99	0.000	0.000	2.778	30.00	Zadar
B10-MP3	Apr 6 /11 11:53:11	13.46	9.652	20.57	0.000	0.000	2.778	20.00	Zadar
B9-MP1	Apr 6 /11 11:54:11	84.33	69.09	79.25	0.000	0.000	2.778	5.000	Zadar
B11-MP3	Apr 6 /11 11:55:11	15.87	10.54	23.75	0.000	0.000	2.778	25.00	Zadar
B9-MP2	Apr 6 /11 11:55:11	26.03	46.74	87.12	0.000	0.000	2.778	10.000	Zadar

B9-MP6	Apr 6 /11 11:55:11	6.477	4.826	11.18	0.000	0.000	2.778	30.00	Zadar
B9-MP5	Apr 6 /11 11:55:11	8.509	5.461	9.017	0.000	0.000	2.778	25.00	Zadar
B10-MP1	Apr 6 /11 11:56:11	12.19	21.34	21.34	0.000	0.000	2.778	10.000	Zadar
B10-MP2	Apr 6 /11 11:57:11	12.57	11.05	12.19	0.000	0.000	2.778	15.00	Zadar
B10-MP6	Apr 6 /11 11:57:11	3.556	3.556	9.398	0.000	0.000	2.778	35.00	Zadar
B10-MP5	Apr 6 /11 11:57:11	2.413	5.080	7.493	0.000	0.000	2.778	30.00	Zadar
B11-MP1	Apr 6 /11 11:58:11	21.34	28.45	16.76	0.000	0.000	2.778	15.00	Zadar
B11-MP2	Apr 6 /11 11:59:11	14.22	3.175	18.16	0.000	0.000	2.778	20.00	Zadar
B11-MP6	Apr 6 /11 11:59:11	2.667	3.683	10.80	0.000	0.000	2.778	40.00	Zadar
B11-MP5	Apr 6 /11 11:59:11	3.302	3.810	10.41	0.000	0.000	2.778	35.00	Zadar
B9-MP8	Apr 6 /11 11:43:11	3.937	4.064	8.382	0.000	0.000	2.778	40.00	Zadar
B10-MP8	Apr 6 /11 11:45:11	3.937	2.032	7.493	0.000	0.000	2.778	45.00	Zadar
B11-MP8	Apr 6 /11 11:47:11	4.191	2.032	9.652	0.000	0.000	2.778	50.00	Zadar
B12-MP1	Sep 9 /95 10:22:10	38.23	29.97	62.10	0.000	0.000	2.778	10.000	Zadar
B13-MP1	Sep 9 /95 10:24:10	15.75	15.37	29.46	0.000	0.000	2.778	15.00	Zadar
B14-MP1	Sep 9 /95 10:26:10	16.38	15.11	13.59	0.000	0.000	2.778	20.00	Zadar
B12-MP6	May 13 /11 10:32:10	4.064	2.159	4.318	0.000	0.000	2.778	60.00	Zadar
B13-MP6	May 13 /11 10:35:10	2.159	1.016	2.540	0.000	0.000	2.778	65.00	Zadar
B14-MP6	May 13 /11 10:37:10	1.651	1.016	2.540	0.000	0.000	2.778	70.00	Zadar
B12-MP3	May 13 /11 10:39:10	4.763	4.509	8.636	0.000	0.000	2.778	30.00	Zadar
B13-MP3	May 13 /11 10:41:10	2.794	2.730	5.525	0.000	0.000	2.778	35.00	Zadar
B14-MP3	May 13 /11 10:44:10	2.730	2.032	3.810	0.000	0.000	2.778	40.00	Zadar
B12-MP5	May 13 /11 10:45:10	3.175	2.413	3.937	0.000	0.000	2.778	50.00	Zadar
B13-MP5	May 13 /11 10:47:10	2.413	1.524	2.540	0.000	0.000	2.778	55.00	Zadar
B12-MP2	May 13 /11 10:48:10	7.366	9.144	8.382	0.000	0.000	2.778	20.00	Zadar
B12-MP4	May 13 /11 10:49:10	16.38	10.16	10.16	0.000	0.000	2.778	40.00	Zadar
B14-MP5	May 13 /11 10:50:10	1.778	1.016	1.905	0.000	0.000	2.778	60.00	Zadar
B12-MP2	May 13 /11 10:50:10	7.620	7.620	8.382	0.000	0.000	2.778	25.00	Zadar
B13-MP4	May 13 /11 10:51:10	24.00	16.13	16.51	0.000	0.000	2.778	45.00	Zadar
B14-MP2	May 13 /11 10:53:10	5.842	5.906	7.112	0.000	0.000	2.778	30.00	Zadar
B14-MP4	May 13 /11 10:54:10	17.65	12.70	12.32	0.000	0.000	2.778	50.00	Zadar
B12-MP7	May 13 /11 10:32:10	2.667	0.762	1.905	0.000	0.000	2.778	70.00	Zadar
B13-MP7	May 13 /11 10:35:10	2.032	0.635	1.397	0.000	0.000	2.778	75.00	Zadar
B14-MP7	May 13 /11 10:37:10	1.270	0.508	0.762	0.000	0.000	2.778	80.00	Zadar
B15-MP5	Oct 5 /11 10:25:10	4.318	3.556	3.175	0.000	0.000	2.778	25.00	Zadar
B16-MP5	Oct 5 /11 10:26:10	5.080	4.953	4.953	0.000	0.000	2.778	20.00	Zadar
B17-MP5	Oct 5 /11 10:28:10	12.32	16.89	15.75	0.000	0.000	2.778	15.00	Zadar
B15-MP2	Oct 5 /11 11:24:11	22.35	18.16	8.382	0.000	0.000	2.778	12.50	ZADAR
B15-MP3	Oct 5 /11 11:24:11	25.64	19.37	20.03	0.000	0.000	2.778	15.00	ZADAR
B15-MP4	Oct 5 /11 11:24:11	14.86	14.60	16.64	0.000	0.000	2.778	20.00	ZADAR
B16-MP2	Oct 5 /11 11:26:11	22.35	15.75	14.48	0.000	0.000	2.778	7.500	ZADAR
B16-MP3	Oct 5 /11 11:26:11	0.000	26.27	25.21	0.000	0.000	2.778	10.000	ZADAR
B16-MP4	Oct 5 /11 11:26:11	9.652	19.18	12.83	0.000	0.000	2.778	15.00	ZADAR
B17-MP3	Oct 5 /11 11:27:11	120.5	202.8	163.4	0.000	0.000	2.778	5.000	ZADAR
B17-MP2	Oct 5 /11 11:27:11	0.000	239.3	0.000	0.000	0.000	2.778	2.500	ZADAR
B17-MP4	Oct 5 /11 11:27:11	20.32	81.41	37.72	0.000	0.000	2.778	10.000	ZADAR
B15-MP1	Oct 5 /11 11:24:11	11.68	28.19	18.54	0.000	0.000	2.778	11.50	ZADAR
B16-MP1	Oct 5 /11 11:26:11	26.92	56.77	38.23	0.000	0.000	2.778	6.500	ZADAR
B17-MP1	Oct 5 /11 11:27:11	217.6	0.000	237.6	0.000	0.000	2.778	1.500	ZADAR

Fig. 7. Record listing

TABLE 6

95% confidence line equations for each section of measurement setup

Section	Distance from blast (m)	95% confidence line equation
1	18-35	$PPV = 341(SD)^{-0.826}$
2	35+	$PPV = 58806(SD)^{-2.397}$
3	40+	$PPV = 417410(SD)^{-2.966}$
4	45+	$PPV = 12478448(SD)^{3,929}$

TABLE 7

Calculated scaling distances for each section for velocity limit of 40 mm/s

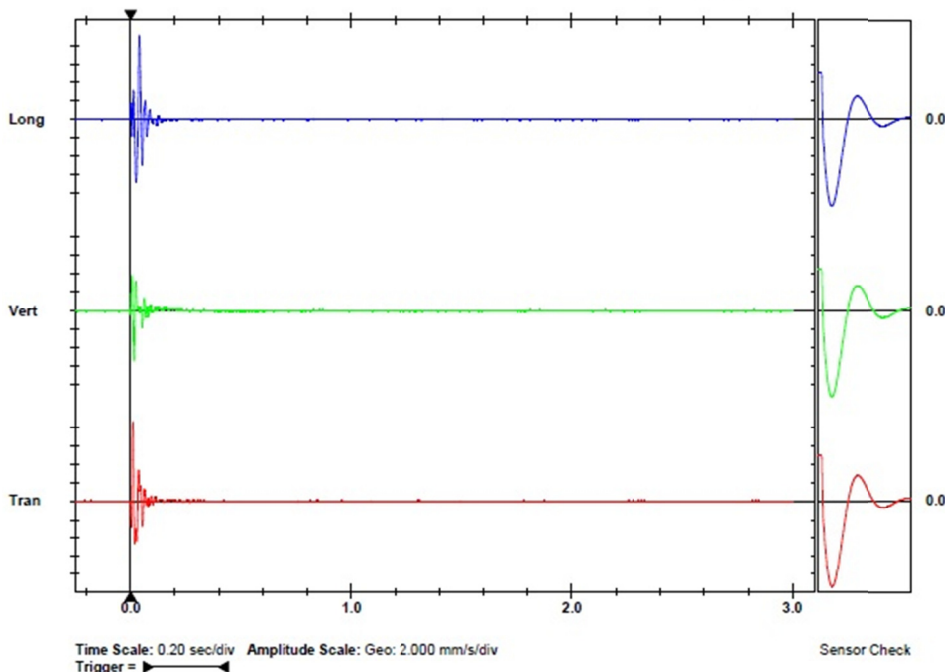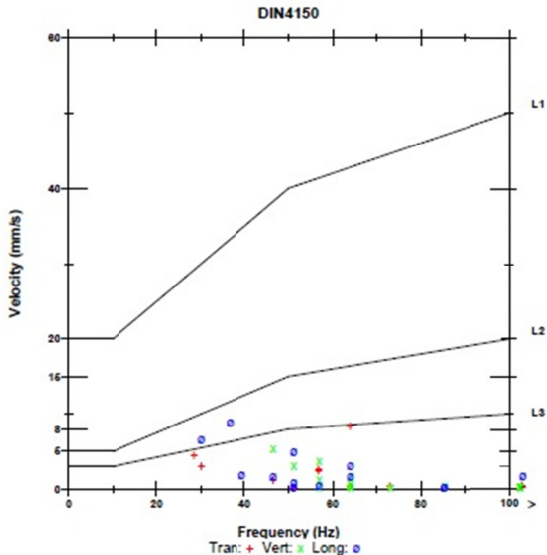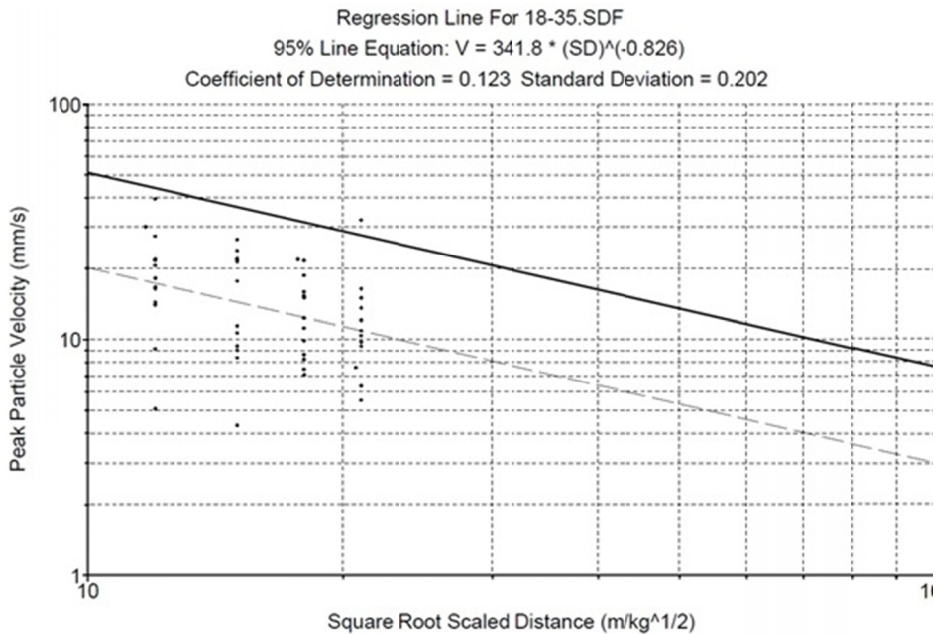| PPV	SD (m/kg$^{1/2}$)			
(mm/s)	18-35	35+	40+	45+
40	13.4	21.0	22.6	25.0

602

Fig. 8. Sample of the event report

Fig. 9. Graphical presentation of peak particle velocity components and square root scaled distance
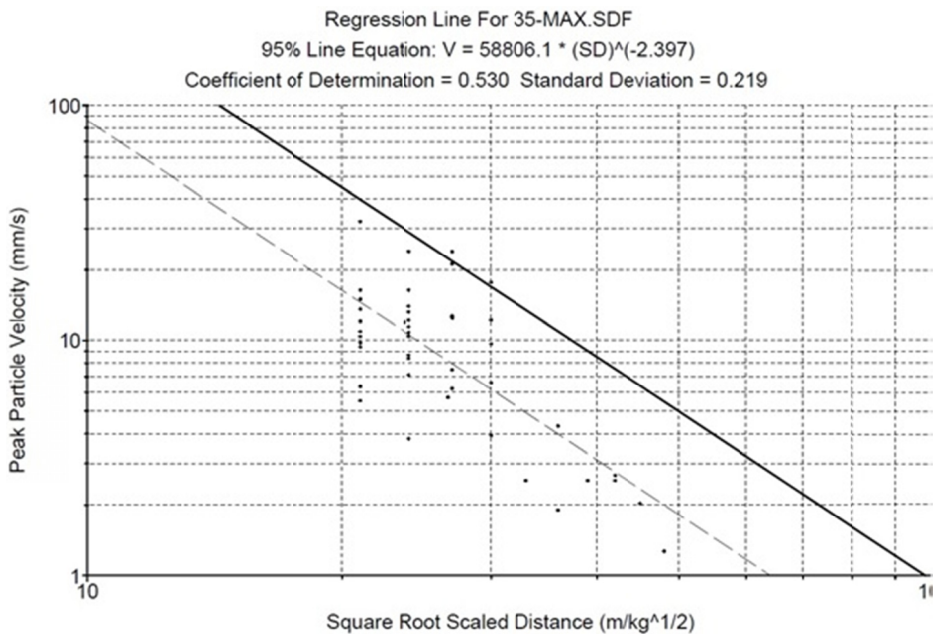for section 18-35m with 95% confidence line equation

Fig. 10. Graphical presentation of peak particle velocity components and square root scaled distance
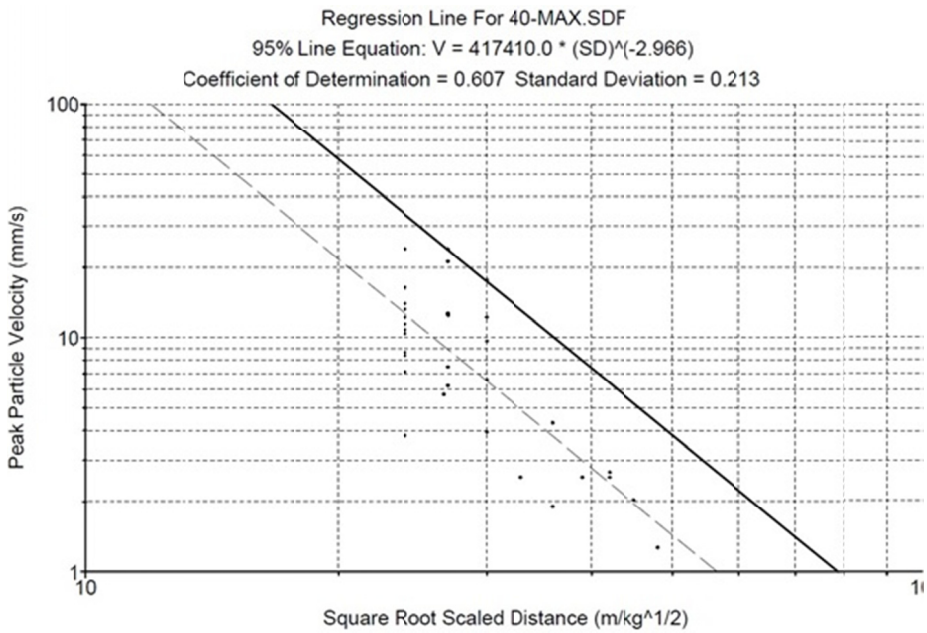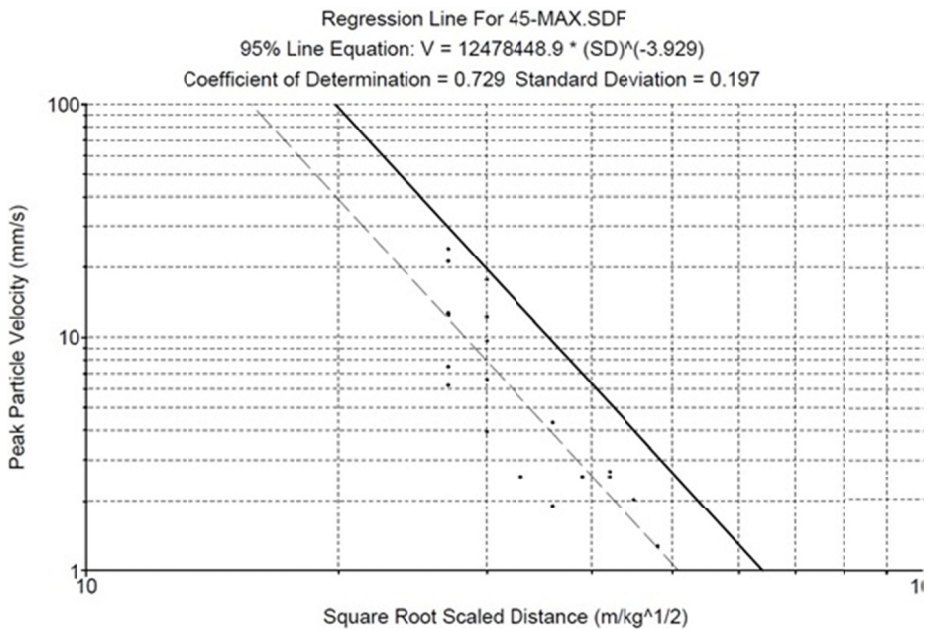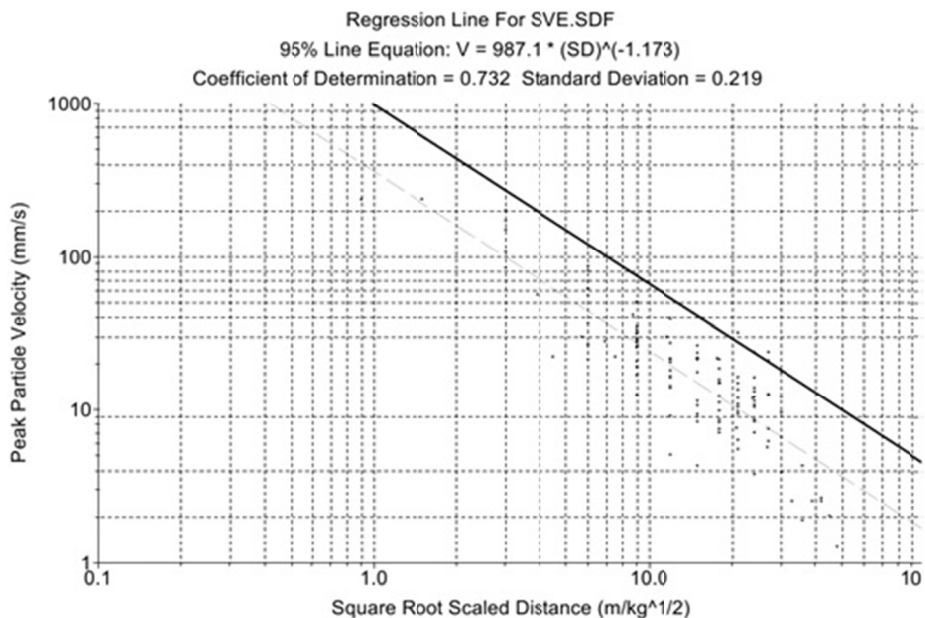for section 35 m+ with 95% confidence line equation

604

Fig. 11. Graphical presentation of peak particle velocity components and square root scaled distance for section 40 m+ with 95% confidence line equation

Fig. 12. Graphical presentation of peak particle velocity components and square root scaled distance for section 45 m+ with 95% confidence line equation

Regression Line For SVE.SDF
95% Line Equation: V = 987.1 * (SD)^(-1.173)
Coefficient of Determination = 0.732 Standard Deviation = 0.219

Fig. 13. Graphical presentation of peak particle velocity components and square root scaled distance for all test blasts with 95% confidence line equation
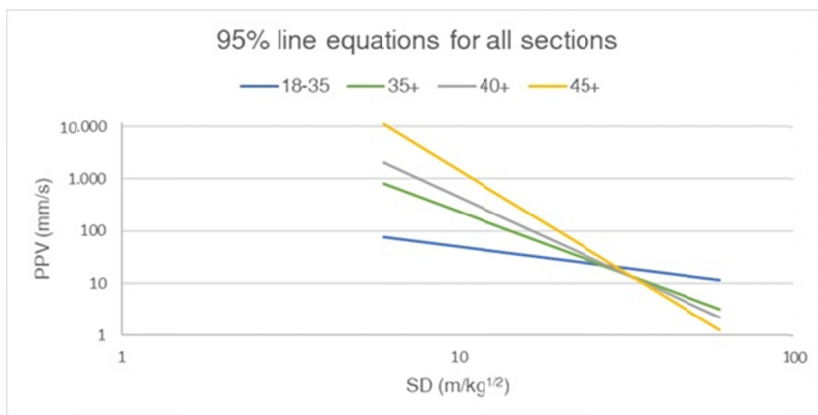
Fig. 14. Graphical presentation of 95% confidence line equations for all sections

Hence, if section 4 (45+ meter from the blast) is used in calculation for permitted charge weight per delay in relation to distance, the results will give largely reduced permitted charge weight per delay. For the end user it means increase in expenses for drilling and blasting works.

All these differences happen due to regression curve approximation for the area not covered by monitoring instruments.
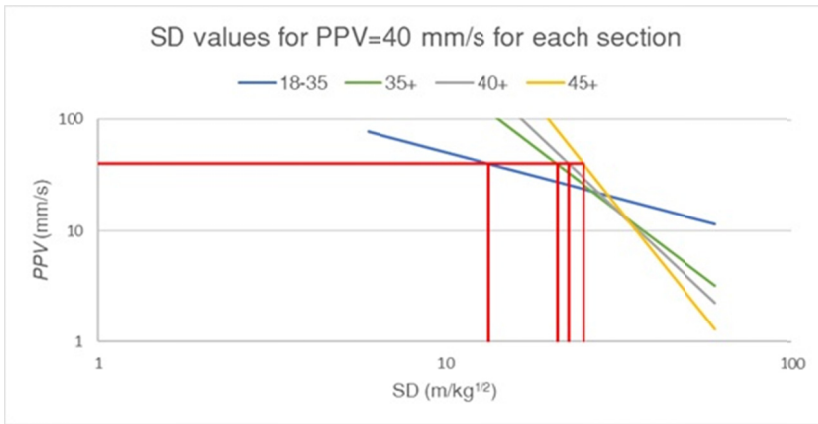
Fig. 15. Graphical presentation of scaling distances for each section and velocity limit of 40 mm/s

TABLE 8

Calculated permitted charge weight per delay for each section for velocity limit of 40 mm/s

R (m)	Charge weight per delay for PPV 40 mm/s						
	18-35	35+		40+		45+	
		kg	%	kg	%	kg	%
10	0.6	0.2	41.1	0.2	35.1	0.2	28.8
20	2.2	0.9	41.0	0.8	35.1	0.6	28.8
30	5.0	2.0	41.0	1.8	35.1	1.4	28.8
40	8.9	3.6	41.0	3.1	35.1	2.6	28.8
50	13.9	5.7	41.0	4.9	35.1	4.0	28.8
100	55.6	22.8	41.0	19.5	35.1	16.0	28.7
150	124.9	51.2	41.0	43.9	35.1	35.9	28.8
200	222.0	91.1	41.0	78.0	35.1	63.9	28.8

6. Conclusion

It has been proven that any prediction model, among other factors, highly depends on positioning of vibration monitoring instruments. When fitting of experimental $SD - PPV$ data with best fit curve and 95% confidence line to equation (1), it gives the coefficients H and β which are valid only for the scaled distance (SD) range used for fitting. Extrapolation outside of this range gives erroneous results. Using the specific prediction model, to predetermine optimal positioning of vibration monitoring instruments was verified to be vital. Depending on vibration monitoring instrument positions, different 95% confidence line equations are calculated. When comparing these equations, the largest differences are closer to the source of explosion. The same occurs when comparing scaling distance for each section equation for the same charge weight per delay and PPV limit. Implementing equations for each section in further calculations for permitted charge weight per delay in relation to distance from the blast, the results show that each section that is further away, gives lower values for charge weight per delay. Hence, as the

vibration monitoring instruments are further away from calculated optimal position, the drilling and blasting works grow more expensive.

This paper gives recommendation for vibration monitoring instruments positioning during test blast on any new site. Optimal positioning of instruments gives end user measured data needed to perform a reliable calculation for charge weight per delay in relation to distance or scaled distance. This will consequently optimize quantity of explosive used without increasing the possibility of damaging surrounding structures.

Acknowledgements

Reference

Ak H., Iphar M., Yavuz M., Konuk A., 2009. *Evaluation of ground vibration effect of blasting operations in a magnesite mine*. Soil Dyn. Earthq. Eng. **29**, 669-676.

Badal K.K., 2010. B*last Vibration Studies in Surface Mines*. 41.

Croatian Standards Institute, 2011. DIN 4150 Vibracije u građevinama – 3. dio: Djelovanje na konstrukcije. Croatian Standards Institute, Zagreb.

Dowding C.H., 1985. *Blast vibration monitoring and control*.

I.G.I., 1967. Osnovna geološka karta, tumač za list Zadar L 33-139. Institut ZA Geološka Istraživanja Zagreb, Beograd.

Instantel Inc. (2013) Instantel Minimate Plus Datasheet. In: Specto Technol. https://www.spectotechnology.com/download/minimate-plus-datasheet-instantel/?wpdmdl=1247.

Instantel Inc. (2004) Blastware Operator Manual. Instantel.

ISEE (1998) Blasters' Handbook.

Kumar R., Choudhury D., Bhargava K., 2016. *Determination of blast-induced ground vibration equations for rocks using mechanical and geological properties*. J. Rock Mech. Geotech. Eng. **8** 341-349. doi: 10.1016/j.jrmge.2015.10.009.

Kuzmenko A.A., Vorobev V.D., Denisyuk I.I., Dauetas A.A., 1993. *Seismic effects of blasting in rock*.

MAXAM Hrvatska d.o.o. (2010) ELEXIT gelatinous dynamite catalogue. 2.

Mesec J., Kovač I., Soldo B., 2010. *Estimation of particle velocity based on blast event measurements at different rock units*. Soil Dyn. Earthq. Eng. **30**, 1004-1009. doi: 10.1016/j.soildyn.2010.04.011.

Monjezi M., Ahmadi M., Sheikhan M., Bahrami A., Salimi A.R., 2010. *Predicting blast-induced ground vibration using various types of neural networks*. Soil Dyn. Earthq. Eng. **30**, 1233-1236. doi: 10.1016/j.soildyn.2010.05.005.

Nicholson R.F., 2005. *MASTER'S THESIS Determination of Blast Vibrations Using Peak Particle Velocity at Bengal Quarry, in St Ann, Jamaica A case study*. Dept. Civ. Environemntal Eng. Lulea Univ. Technol. **1**, 51-53.

Ozer U., 2008. *Environmental impacts of ground vibration induced by blasting at different rock units on the Kadikoy-Kartal metro tunnel*. Eng. Geol. **100**, 82-90.

Rai R., Shrivastva B.K., Singh T.N., 2005. *Prediction of maximum safe charge per delay in surface mining*. Min. Technol. **114**, 227-231.

Resende R., Lamas L., Lemos J., Calçada R., 2014. *Stress wave propagation test and numerical modelling of an underground complex*. Int. J. Rock Mech. Min. Sci. **72**, 26-36. doi: 10.1016/j.ijrmms.2014.08.010.

Siskind D.E., 2000. *Vibrations from blasting*.